Extreme Mechanics Letters 40 (2020) 100978

Contents lists available at ScienceDirect

Extreme Mechanics Letters

journal homepage: www.elsevier.com/locate/eml

Cracks outrun erosion in degradable polymers

Meixuanzi Shi [a,b], Jason Steck [a], Xuxu Yang [a,c], Guogao Zhang [a,c], John Yin [a], Zhigang Suo [a,*]

[a] John A. Paulson School of Engineering and Applied Science, Kavli Institute for Nanobio Science and Technology, Harvard University, Cambridge, MA 02138, USA

[b] State Key Laboratory for Strength and Vibration of Mechanical Structures, Department of Engineering Mechanics, Xi'an Jiaotong University, Xi'an 710049, China

[c] State Key Laboratory of Chemical Engineering, College of Chemical and Biological Engineering, Zhejiang University, Hangzhou 310027, China

ARTICLE INFO

Article history:
Received 22 June 2020
Received in revised form 27 August 2020
Accepted 6 September 2020
Available online 12 September 2020

Keywords:
Degradable polymer
Elastomer
Stress corrosion
Environmental stress cracking
Slow crack growth

ABSTRACT

Degradable polymers are being developed for medical applications and environmental sustainability. The molecular mechanism of degradation is known: a polymer dissociates in response to a trigger, such as light, water, or biomolecules. However, the spatial and temporal processes of degradation are poorly characterized. Here we show that degradation can be highly heterogeneous, and can readily lead to cracks that outrun erosion in speed by orders of magnitude. This paper studies crack growth in poly(glycerol sebacate) (PGS), a degradable elastomer developed for medical applications. The elastomer is a polyester in which ester bonds hydrolyze in the presence of water molecules. We prepare a sample of PGS with a precut crack, apply various loads, and record the crack growth using a camera. A small load opens a crack in PGS, and provides a path for water molecules to reach the crack tip, possibly by clearing the hydrophobic debris of reaction products, enabling hydrolysis at the crack tip to outrun elsewhere. We show that the speed of the hydrolytic crack depends on relative humidity, pH, and applied load. In a fixed environment, we identify two regimes of crack growth: one is sensitive to the magnitude of the applied load, and the other is not. The hydrolytic crack causes the polymer to lose its load-carrying capacity prematurely, and fragmented polymer particles can cause severe medical complications.

1. Introduction

Degradable polymers are used in surgery [1,2], drug delivery [3–6], and tissue engineering [7–9]. Degradable polymers are also being developed for environmental sustainability [10–13]. Nearly a century of use of non-degradable polymers has harmed the environment; for example, the oceans will soon be populated by more plastics than fish, and become "plastic oceans" [14].

A polymer degrades by a complex process in space and time. At the molecular scale, atomic bonds break in response to a trigger, such as light, water, and biomolecules. The kinetics of bond cleavage, or the degradation kinetics, can be significantly affected by properties of the surrounding environment [15]. Examples include cellulose degrading more rapidly at higher relative humidities [16], and the reaction mechanism of poly(lactic-co-glycolic acid) changing from bulk erosion at low pH to surface erosion at high pH [17]. After dissociation, polymer chains detach from the material and diffuse into the surroundings. Polymer chains may shed by volume or surface erosion, dictated by the rates of diffusion and reaction [18–21]. Volume erosion consists of homogeneous dissociation of polymer chains throughout the material, whereas surface erosion consists of homogeneous dissociation across the surfaces of the material. However, degradation is commonly observed to be heterogeneous, forming cracks and voids [21]. Such morphological changes fit neither volume nor surface erosion.

When a load is applied to a material, a crack concentrates stress at the crack tip. If the material is exposed to a corrosive environment, then stress at the crack tip can lead to crack growth even when the magnitude of the load is small. This phenomenon, commonly called stress corrosion cracking, can lead to unexpected and catastrophic fracture of a material. Stress corrosion cracks have been observed in many materials, including silica glass [22,23], metals [24,25], natural rubber [26], non-degradable polymers [27], and conductive polymers [28], but have not been studied in degradable polymers. We expect that, since degradable polymers corrode in response to a trigger, degradable polymers will suffer stress corrosion cracking.

This paper begins the study of stress corrosion cracking in degradable polymers. Here we show that degradation can be highly heterogeneous, and that, subject to a small mechanical load, the speed of a crack can be orders of magnitude higher than the speed of surface erosion. We choose poly(glycerol sebacate)

* Corresponding author.
E-mail address: suo@seas.harvard.edu (Z. Suo).

https://doi.org/10.1016/j.eml.2020.100978
2352-4316/

(PGS) as a model degradable polymer. We prepare a sample of PGS with a crack, apply various loads, and record the crack growth using a camera. To study the effect of the environment on stress corrosion cracking, we measure crack speed as a function of relative humidity and pH. We find that the crack speed increases with increased humidity and decreased pH. In a fixed environment, we identify two regimes of crack growth: one is sensitive to the magnitude of the applied load, and the other is not. We interpret these regimes of crack growth in context of existing literature on stress corrosion cracking. In practice, the surfaces of degradable polymers will inevitably contain crack-like flaws. Since many applications require these materials to carry loads, it is possible that stress corrosion cracking of degradable polymers is already widespread.

2. Materials and methods

This paper reports that cracks outrun erosion in poly(glycerol sebacate) (PGS) in the presence of water molecules, at room temperature, subject to a small mechanical load. The speed of a crack can be orders of magnitude higher than the speed of surface erosion. PGS and its derivatives have been developed for drug delivery and the regeneration of nerve and bone tissues [6,9,29–32]. PGS is a three-dimensional polyester network formed through the condensation of glycerol and sebacic acid molecules (Fig. 1). A sebacic acid molecule has two –COOH groups, and a glycerol molecule has three –OH groups. The two species of molecules can condense into a polyester chain, producing water molecules and leaving one –OH group on every glycerol monomer available for chemical coupling. This –OH group on a glycerol monomer and a sebacic acid monomer can also condense into an ester bond, forming a branch. Fig. 1 shows two PGS polymer chains crosslinked by a single sebacic acid molecule. Other possibilities include two polyester chains connected by a PGS polymer, multiple crosslinks between two PGS polymers, and defects such as loops and dangling chains. PGS degrades through hydrolysis of the ester bonds. Condensation and hydrolysis are reactions in opposite directions.

We synthesize PGS in two steps. First, we melt the solid sebacic acid and mix it with glycerol at a 1:1 ratio, in a N_2 atmosphere, at 120 °C for 24 h. At the end of this step, reactants are partially polymerized and remain a liquid. Second, we pour the mixture into a mold to form an elastomer in a vacuum oven (VWR symphony Vacuum Oven), at 120 °C for 48 h, after gently decreasing pressure to vacuum for 5h. Once the samples are returned to ambient temperature and relative humidity, hydrolysis prevails, and degradation begins.

We characterize the mechanical behavior of PGS by measuring the shear modulus, work of fracture, and toughness. We test samples with and without precut cracks [33]. A rectangular PGS sample without precut crack is gripped with two rigid clamps, with the exposed sample having length 10 cm, height 1 cm, and thickness 3 mm (Fig. 2a). The clamps are pulled by a tensile tester at a constant velocity of 0.5 mm s^{-1}, and the force is recorded as a function of displacement. Define the nominal stress s as the force in the current state divided by the length and thickness of the sample in the undeformed state. Define the strain ϵ as the displacement divided by the height in the undeformed state. The measured stress–strain curve varies appreciably from sample to sample. This variation may be tightened by better control of synthesis, but we have not pursued this matter. For our experimental setup, the small-strain shear modulus μ is calculated according to $s = 4\mu\epsilon$ (see Appendix A). Our measurement gives a shear modulus of 64.08 ± 10.45 kPa. The fracture strain is 0.84 ± 0.3. Define the work of fracture W_f as the work done up to fracture divided by the volume of the sample, as given by the area under the stress–strain curve. Our data give $W_f = (104.6 \pm 28.8) \times 10^3$ J m^{-3}.

A 20 mm crack is cut into the PGS sample with a razor blade, parallel to the clamps (Fig. 2b). Toughness is defined as the energy needed to advance the crack per unit area. The sample is elongated to a strain ϵ, and the energy release rate is $G = HW(\epsilon)$, where H is the height of the sample in the undeformed state, and $W(\epsilon)$ is the work per unit volume of the PGS sample without a crack. When the sample with a crack ruptures, the energy release rate is calculated at the critical strain, and this critical energy release rate gives the toughness. The measured toughness is 432 ± 73.1 J m^{-2}. This is perhaps the first time that the toughness of any degradable elastomer is reported. The value should be compared to common elastomers, such as PDMS (∼300 J/m^2) [34] and natural rubber (∼10^4 J/m^2) [35]. Since the crack length is similar to the sample height in our experiments, it is possible that the energy release rate is a function of the crack length, which may introduce error into our measurements [33]. This possible error may be reduced by decreasing the sample height or increasing the precut crack length, but we have not pursued this matter.

The toughness assesses the resistance of a material to fracture in the presence of crack-like flaws, which may lead to rupture at stresses far below the strength of a pristine sample. Indeed, some of our samples without precut cracks rupture at the same stretch as those samples that do have precut cracks (Fig. 2a). All samples have defects, but if a flaw is smaller than the fractocohesive length, then the strength of the sample will not be reduced [36]. For PGS, we estimate the fractocohesive length to be $\Gamma/W_f \sim$ 4.1 mm. For our experimental setup, the length scale to compare with the fractocohesive length is the height H of the sample in the undeformed state. We leave this line of thoughts here, and focus our attention on stress corrosion cracking.

3. Results

3.1. Stress corrosion cracking

We next study stress corrosion cracking of PGS in water. We grip a PGS sample (length 10 cm, height 2 cm, and thickness 3 mm) with two rigid clamps, precut a crack (20 mm), and pull the clamps to stretch the sample to a constant strain corresponding to an energy release rate of 19.2 J m^{-2}. This energy release rate is much below the toughness, so that the crack does not advance rapidly. The stretched sample is then submerged in deionized (DI) water, and the crack tip is observed with a camera (Canon EOS 70D and Canon EF 24–105 mm lens, resolution of 0.1 mm) (Fig. 3a). The camera periodically takes a photo of the crack tip. The crack advances slowly, but much more rapidly than the surface erodes (Fig. 3b). The crack velocity is calculated as the crack growth divided by the time between images. The crack length increases linearly with time, indicating a constant crack velocity (Fig. 3c). The average crack velocity is calculated to be 1.15×10^{-6} m s^{-1}. We repeat this experiment with several values of energy release rate (Fig. 3c). The data for all stress corrosion experiments is provided in Table B.1 (Appendix B).

We next study the effect of pH on stress corrosion cracking (Fig. 4). A constant energy release rate is applied to a PGS sample with a precut crack. The stretched samples are submerged in either dilute hydrochloric acid solution at pH 2 or dilute sodium hydroxide solution at pH 12, and the crack length is measured using a camera. The crack growth velocity is much slower in alkaline solution than in acid solution and neutral DI water. At an energy release rate of 29 J m^{-2}, the crack velocity in alkaline solution is 4.6×10^{-7} m s^{-1}, whereas the crack velocity in acidic solution is 1.5×10^{-5} m s^{-1}, approximately 33 times slower. We

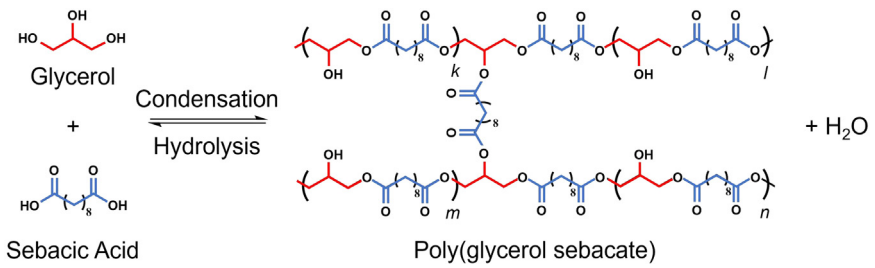

Fig. 1. Synthesis and degradation of PGS. PGS is synthesized through condensation of hydroxyl groups on glycerol and carboxylic acid groups on sebacic acid, producing ester bonds and water molecules. PGS degrades through hydrolysis of the ester bonds in the presence of water molecules.

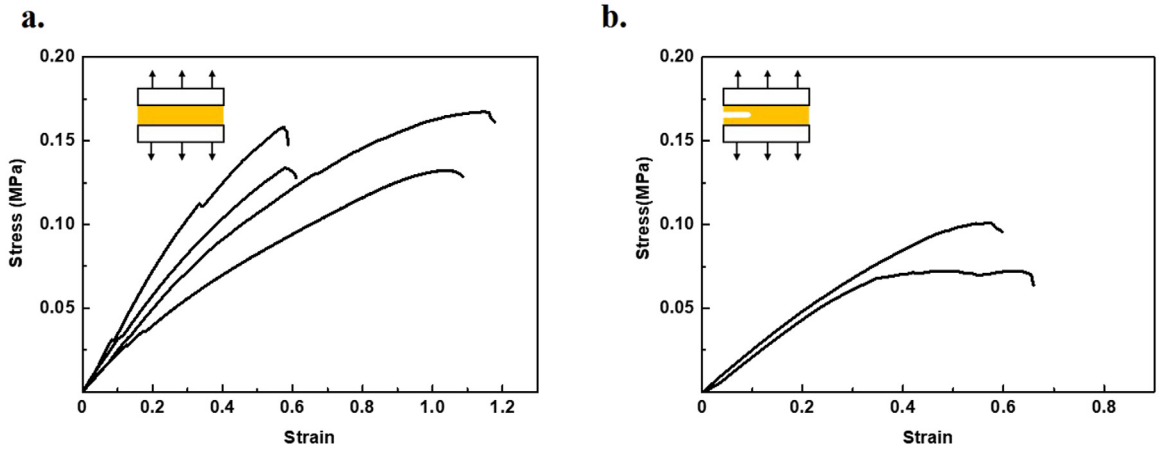

Fig. 2. Stress–strain curve and toughness. a. A PGS sample is gripped between two rigid clamps, stretched at a constant velocity, and the stress is measured. b. A crack is cut into an identical PGS sample with a razor blade. The notched sample is stretched at a constant velocity, and the critical strain at the onset of crack propagation is measured. Each curve represents a separate sample and test.

interpret these findings to mean that hydronium ions catalyze the hydrolysis of the ester bonds.

The crack velocity is also accelerated by an applied load for all solutions. When the applied load is low, the crack will seem to shrink in photos rather than propagate due to the swelling, leading to the negative crack velocity. This observation indicates that, for a given environment, a threshold of energy release rate exists, below which the crack does not outrun erosion.

We now study the effect of humidity on stress corrosion cracking. A constant energy release rate is applied to a PGS sample with a precut crack. The stretched samples are left in an ambient environment of 10% relative humidity, and the crack length is measured using a camera (Fig. 5). The crack advances ahead of the surfaces of the bulk material, indicating stress-assisted degradation at the crack tip. At an energy release rate of 22.5 J m^{-2}, the crack velocity in air is measured to be 2.28×10^{-7} m s^{-1}. This crack velocity is ∼20 times slower than the equivalent test in DI water, where the crack velocity at an energy release rate of 19.2 J m^{-2} is 1.15×10^{-6} m s^{-1}. The difference between crack growth in humid air and in liquid water is understood by considering the concentration of water molecules at the crack tip, where liquid water will provide greater availability of water molecules to hydrolyze ester bonds.

3.2. Regimes of crack growth

In the absence of mechanical load, PGS degrades through surface erosion [29]. It was reported that a rectangular sample, sides 5 mm, 5 mm, and 2 mm, after being submerged in a PBS solution for 60 days, lost mass by 17%. We use this observation to estimate the erosion speed as follows. The initial sample has a surface area of 90 mm^2, and a volume of 50 mm^3. The loss of mass is taken to correspond to a loss of volume of 8.5 mm^3. This loss of mass corresponds to erosion of a layer of thickness of 0.094 mm. We further assume that the surface erosion is linear in time, and estimate the erosion speed to be $\sim 1.82 \times 10^{-11}$ m s^{-1}.

This estimated erosion speed is two orders of magnitude lower than the crack speed that we measured at the lowest energy release rate for a sample submerged in DI water. This difference may be caused by several factors. (1) PBS has a buffered pH of 7.4. We have shown that degradation is slower at higher pH. Therefore, the crack speed in DI water should be faster than the erosion speed for a sample in PBS. We have not studied the effect of other ions, if any, on crack speed. (2) The crack removes debris of the reaction products by advancing into the material. Even a small energy release rate opens the crack to a displacement much larger than the size of a water molecule. The removal of debris will increase the crack velocity above the erosion velocity. (3) When the stretch is small, the crack propagation distance is too small to detect by comparing photos. In this circumstance, the error in the measured results is large.

When PGS is in a given environment, such as in DI water, the crack speed is a function of energy release rate (Fig. 6a). To plot this figure, we have used the data determined in our measurements (Fig. 3c). Also included is the speed of surface erosion estimated above. At small values of energy release rate, the crack speed increases steeply with energy release rate. The crack speed reaches $\sim 2 \times 10^{-5}$ m s^{-1} at an energy release rate of 50 J m^{-2}, six orders of magnitude greater than that of erosion. At an energy release rate of ∼70 J m^{-2}, the crack speed plateaus at $\sim 2 \times 10^{-4}$ m s^{-1}, and becomes insensitive to the magnitude of the energy release rate. Once the energy release rate equals the toughness, rupture proceeds by fast fracture, which is unrelated to hydrolysis.

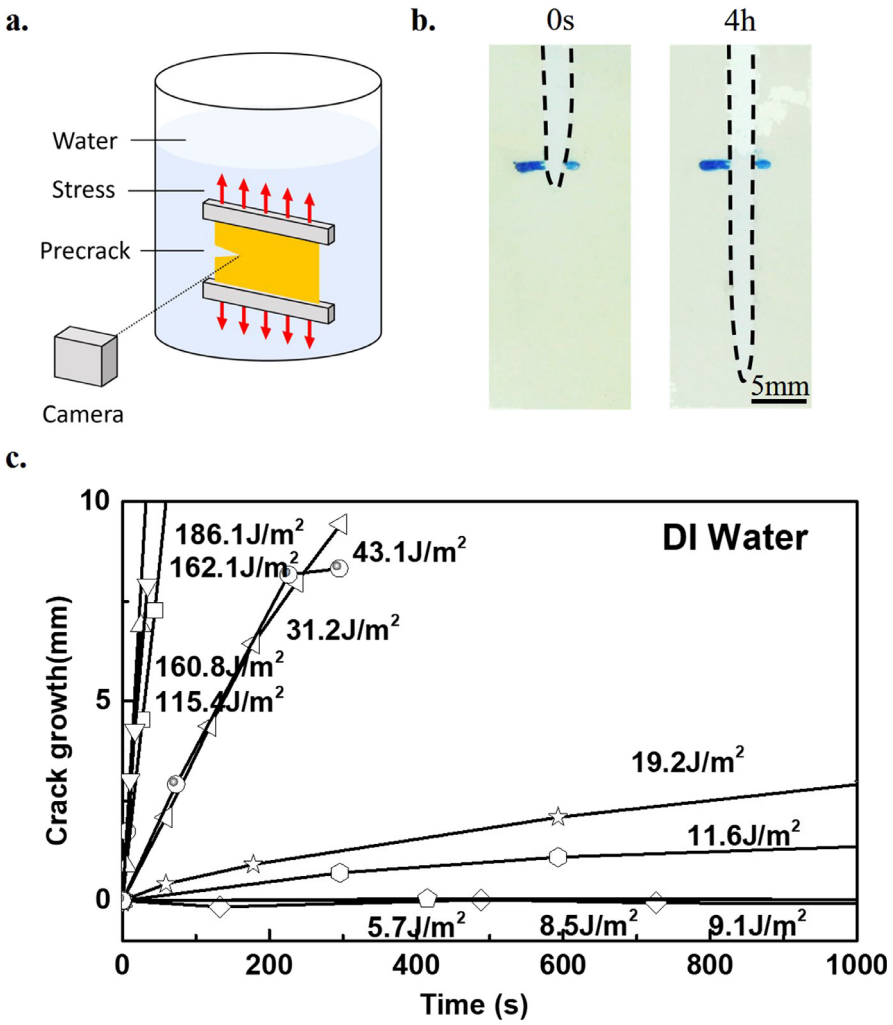

Fig. 3. Stress corrosion cracking in PGS submerged in deionized water. a. A PGS sample is precut with a crack, stretched to a constant strain, submerged in DI water, and observed by a camera. b. At an energy release rate of 19.2 J m^{-2}, the crack advances 3.5 cm in 4 h. c. Crack growth as a function of time, where each line represents a crack advancing in a sample subject to a value of energy release rate.

Similar regimes of crack growth have been documented in the literature for many other materials. In a silica glass, a slow crack grows under applied load in a moist environment [22]. The crack speed increases with energy release rate when the intense stress at the crack tip assists in hydrolysis. The crack speed becomes insensitive to energy release rate when crack growth is rate-limited by the diffusion of water molecules to the crack tip [23]. In natural rubber, a crack advances due to the attack of the carbon–carbon double bonds by ozone, and the crack speed is insensitive to energy release rate [26]. This observation is interpreted as follows. The stress at the crack tip is not intense enough to accelerate the chemical reaction, but the crack opens a path for ozone molecules in the environment to access the polymer chains at the crack tip. In the conductive polymer poly(3,4-ethylenedioxythiophene):poly(styrenesulfonate) (PEDOT:PSS) and the silicone elastomer polydimethylsiloxane (PDMS), in moist environment, crack speed increases with energy release rate [27,28]. Although both PDMS and silica degrade through hydrolysis of siloxane bonds, PDMS does not display a regime of crack growth insensitive to energy release rate. This finding is consistent with the observation that a crack in PDMS opens much more than a crack in silica. Since this crack opening is significantly larger than the size of a water molecule, a sufficient number of water molecules are able to access the polymer chains at crack tip, and the crack speed is insensitive to the value of energy release rate [27]. In all cases, the interplay between the stress-assisted reaction and the transport of reactive species to the crack tip determines whether the crack speed will be sensitive or insensitive to the value of energy release rate.

We now interpret the experimental data for PGS. In the regime where the crack speed is sensitive to the value of energy release rate, the crack tip blunts and sufficient water molecules are present for the reaction to proceed through stress-assisted hydrolysis (Fig. 6b). No debris impedes liquid water from reaching the crack tip, and the crack opening displacement is $\sim$1 mm (Fig. 6c). In contrast, in the regime where the crack speed is insensitive to the value of energy release rate, a zone of debris develops behind the crack tip (Fig. 6d). The zone of debris is on the order of 3 mm in length (Fig. 6e). Water molecules must diffuse through the debris to reach the crack tip. Taking the diffusivity of water in elastomers, D, to be 10^{-11} m^2 s^{-1} [37], we estimate the time for water to reach the crack tip by $t \sim L^2/D$ to be 10^5 s, where L is the length of the zone of debris. At the plateau crack velocity of $\sim 2 \times 10^{-4}$ m s^{-1}, the crack grows by the length of the zone of debris in 10 s. Since the time scale for diffusion is much longer than that for hydrolysis, we expect that, for energy release rates larger than $\sim$70 J m^{-2}, crack growth is rate-limited by the transport of water to the crack tip. This observation is similar to that reported for a hybrid organic and inorganic molecular network, where bond cleavage of the inorganic network ahead of the crack tip produced

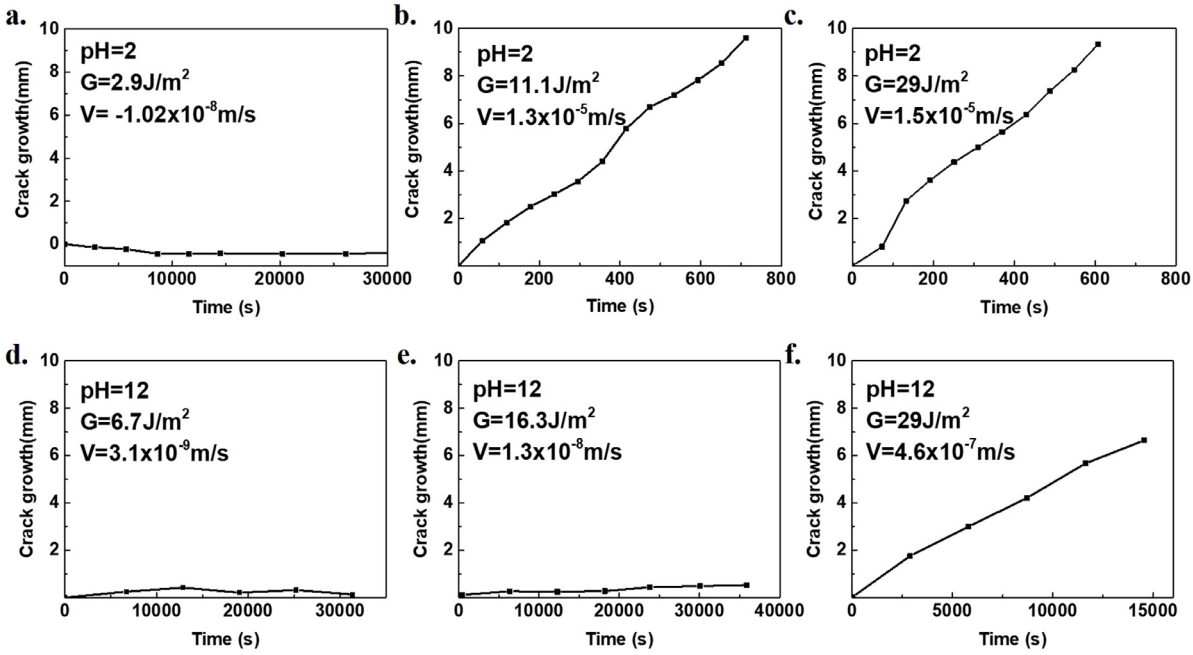

Fig. 4. Effect of pH on crack growth. A PGS sample is submerged in a pH 2 hydrochloric acid solution and a constant energy release rate of a. 2.9 J m^{-2}, b. 11.1 J m^{-2}, and c. 29 J m^{-2} is applied. When the applied load is low, the crack will seem to shrink in photos rather than propagate due to the swelling which leads to the negative crack velocity. A PGS sample is submerged in a pH 12 sodium hydroxide solution and a constant energy release rate of d. 6.7 J m^{-2}, e. 16.3 J m^{-2}, and f. 29 J m^{-2} is applied.

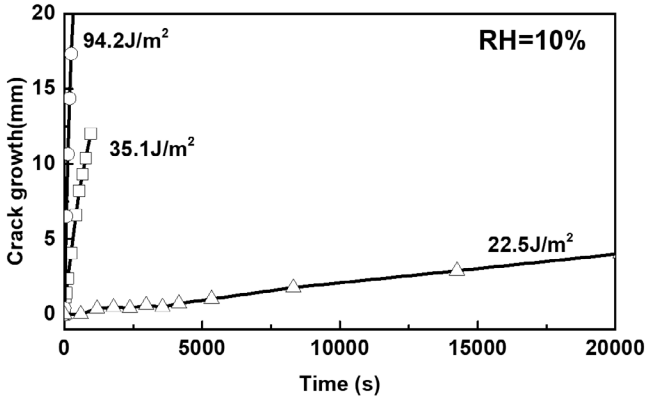

Fig. 5. Effect of humidity on crack growth. A PGS sample with a crack is stretched in open air at a relative humidity of 10%. The crack length is measured as a function of time, and each line represents a constant applied energy release rate. The velocity of the crack is constant in time. A different sample was used for every energy release rate.

a process zone separating the crack tip and the environment [38]. The process zone limits the transport of water to the crack tip and the resulting crack speed is insensitive to the value of energy release rate. In our system, it is possible that high energy release rates separate the crack faces before sufficient bond cleavage has occurred, stretching a sparsely crosslinked process zone at the crack tip. It remains unclear the conditions under which the zone of debris will form.

4. Conclusion

In summary, we demonstrate that cracks outrun erosion in PGS under small loads. The crack velocity depends on pH, humidity, and applied load. For a fixed environment, we observe two regimes of crack growth: one is sensitive to applied load, and the other is not. We propose a mechanism for each regime. Our findings suggest that other degradable polymers should also be susceptible to stress corrosion cracking, and thus call for action. Applications of degradable polymers in medicine and sustainability both require control of the mechanical properties and morphology of the material throughout its lifetime. In medicine, cracks may cause fragmentation, leading to complications, possibly fatal. In sustainability, premature fracture of a material can reduce its lifetime and performance. Furthermore, this study opens immediate opportunities to create degradable polymers that either resist stress corrosion cracking, or encourage it in useful ways.

Declaration of competing interest

The authors declare that they have no known competing financial interests or personal relationships that could have appeared to influence the work reported in this paper.

Acknowledgments

This work was supported by MRSEC, USA (DMR-14-20570). M. Shi is a visiting student at Harvard University supported by the China Scholarship Council. J. Steck acknowledges support from the National Science Foundation, USA Graduate Research Fellowship under Grant No. DGE1745303.

Appendix A

At very small strains, the stress–strain response of a rubber-like material is linear, and is characterized by the shear modulus, μ. Therefore, the shear modulus of a rubber-like material in pure shear can be determined by measuring the slope of the nominal stress with respect to strain at very small strains. Assume the material follows the Neo-hookean model, where σ_1, σ_2, and σ_3 are

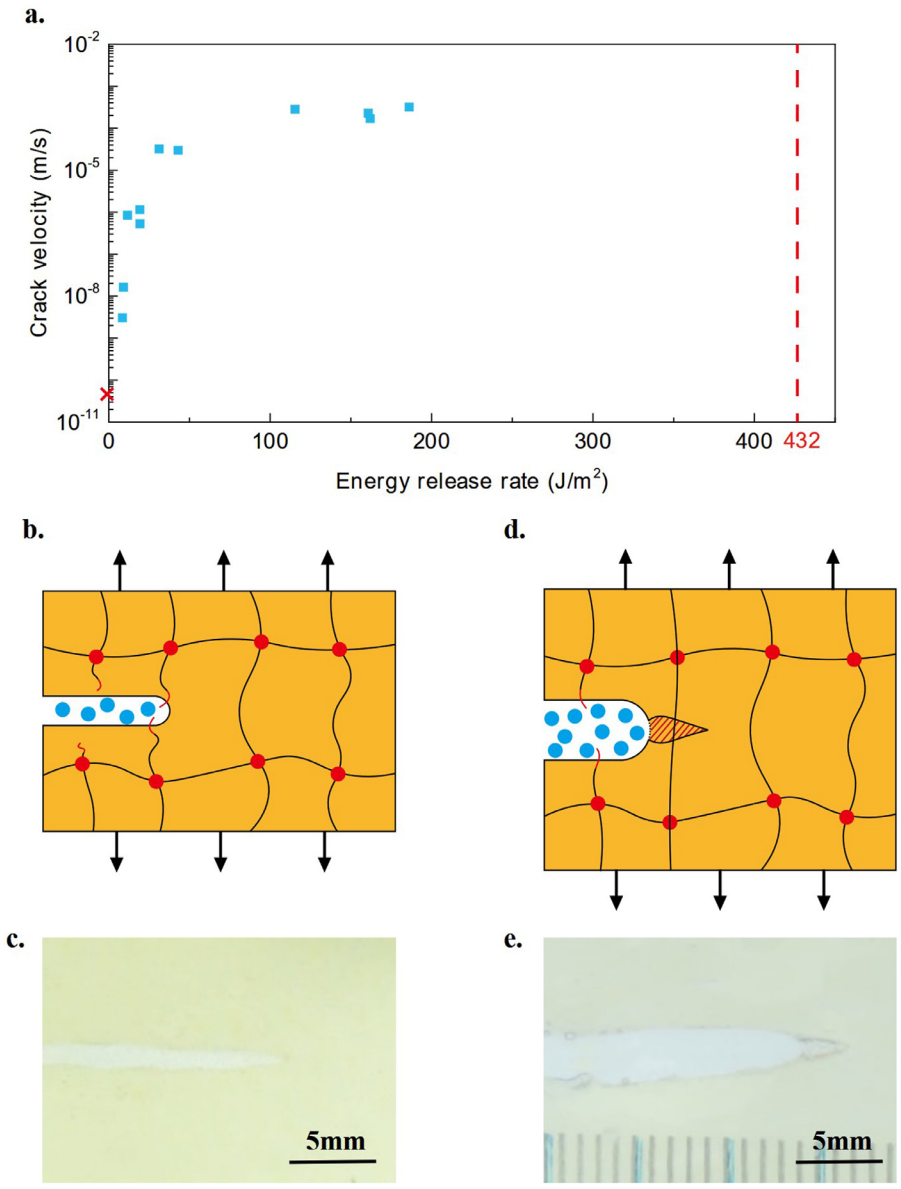

Fig. 6. Crack speed as a function of energy release rate. a. Crack speed in PGS in DI water measured at various values of energy release rate. Each dot corresponds to the speed measured in one sample, i.e., to a line in Fig. 3. b. Illustration and c. image of the regime in which the crack speed is sensitive to the value of energy release rate. The crack tip is fully exposed to water, and stress at the crack tip accelerates the degradation reaction. d. Illustration and e. image of the regime in which the crack speed is insensitive to the energy release rate. A zone of debris emerges, and crack growth is limited by the transport of water through the zone to the crack tip.

the true stresses and λ_1, λ_2, and λ_3 are the stretches in directions 1, 2 and 3, respectively:

$$\sigma_1 - \sigma_3 = \mu(\lambda_1^2 - \lambda_3^2) \tag{A.1}$$

$$\sigma_2 - \sigma_3 = \mu(\lambda_2^2 - \lambda_3^2) \tag{A.2}$$

Define direction 1 along the width, direction 2 along the height, and direction 3 along the thickness of the pure shear sample. Since the thickness is much smaller than the height and width, the sample is in plane stress normal to direction 3: $\sigma_3 = 0$. Since the width is much larger than the height and thickness, the sample is in plane strain normal to direction 1: $\lambda_1 = 1$.

Imposing the incompressibility condition $\lambda_1\lambda_2\lambda_3 = 1$, the stretches are related as $\lambda_3 = \frac{1}{\lambda_2}$. Substituting λ_3 into Eq. (A.2), the true stress in the loading direction is solved for as

$$\sigma_2 = \mu(\lambda_2^2 - \lambda_2^{-2}) \tag{A.3}$$

Next, perform a Taylor expansion of σ_2 centered at $e = 0$, where the stretch is related to engineering strain, e, by $\lambda_2 = 1 + e$:

$$\sigma_2 = \mu(1 + 2e + e^2) - (1 - 2e + 3e^2 + \cdots) \tag{A.4}$$

When the strain is very small, the higher-order strain terms can be neglected, and the true stress is approximately equal to the nominal stress, s. Eq. (A.4) can be simplified as

$$\boldsymbol{s} = 4\boldsymbol{\mu e} \tag{A.5}$$

We interpret μ as the small-strain shear modulus. The small-strain shear modulus is calculated as one quarter of the slope of nominal stress with strain at very small strains.

Appendix B

See Table B.1.

Table B.1
Crack speed, v, as a function of energy release rate, G, in DI water, RH=10%, pH=2 and pH=12.

DI water		RH=10%		pH=2		pH=12	
G (J/m^2)	v (m/s)	G (J/m^2)	v (m/s)	G (J/m^2)	v (m/s)	G (J/m^2)	v (m/s)
5.68	-2.73×10^{-9}	9.08	5.39×10^{-8}	2.89	-1.02×10^{-8}	6.713	3.11×10^{-9}
9.08	1.62×10^{-8}	22.5	2.28×10^{-7}	11.07	1.32×10^{-5}	16.29	1.30×10^{-8}
8.47	3.03×10^{-9}	35.1	1.27×10^{-5}	29.015	1.47×10^{-5}	29.1	4.6×10^{-7}
11.6	8.42×10^{-7}	94.2	5.72×10^{-5}				
19.2	1.15×10^{-6}						
19.4	5.29×10^{-7}						
31.2	3.22×10^{-5}						
43.1	2.96×10^{-5}						
115.4	2.82×10^{-4}						
160.8	2.28×10^{-4}						
162.1	1.70×10^{-4}						
186.1	3.17×10^{-4}						

References

[1] B.D. Ulery, L.S. Nair, C.T. Laurencin, Biomedical applications of biodegradable polymers, J. Polym. Sci. Part B Polym. Phys. 49 (2011) 832–864, http://dx.doi.org/10.1002/polb.22259.

[2] D.K. Gilding, A.M. Reed, Biodegradable polymers for use in surgery—polyglycolic/poly(actic acid) homo- and copolymers: 1, Polymer 20 (1979) 1459–1464, http://dx.doi.org/10.1016/0032-3861(79])90009-0.

[3] W.R. Gombotz, D.K. Pettit, Biodegradable polymers for protein and peptide drug delivery, Bioconjug. Chem. 6 (1995) 332–351, http://dx.doi.org/10.1021/bc00034a002.

[4] B. Amsden, Curable, biodegradable elastomers: emerging biomaterials for drug delivery and tissue engineering, Soft Matter. 3 (2007) 1335–1348, http://dx.doi.org/10.1039/B707472G.

[5] B.G. Amsden, Biodegradable elastomers in drug delivery, Expert Opin. Drug Deliv. 5 (2008) 175–187, http://dx.doi.org/10.1517/17425247.5.2.175.

[6] H.K. Makadia, S.J. Siegel, Poly lactic-co-glycolic acid (PLGA) as biodegradable controlled drug delivery carrier, Polymers 3 (2011) 1377–1397, http://dx.doi.org/10.3390/polym3031377.

[7] L.Y. Lee, S.C. Wu, S.S. Fu, S.Y. Zeng, W.S. Leong, L.P. Tan, Biodegradable elastomer for soft tissue engineering, Eur. Polym. J. 45 (2009) 3249–3256, http://dx.doi.org/10.1016/j.eurpolymj.2009.07.016.

[8] Z. Sheikh, S. Najeeb, Z. Khurshid, V. Verma, H. Rashid, M. Glogauer, Biodegradable materials for bone repair and tissue engineering applications, Materials 8 (2015) 5744–5794, http://dx.doi.org/10.3390/ma8095273.

[9] Poly(glycerol sebacate) in tissue engineering and regenerative medicine, sigma-aldrich, 2020, https://www.sigmaaldrich.com/technical-documents/articles/material-matters/poly-glycerol-sebacate.html. (Accessed 18 June 2020).

[10] R.A. Gross, B. Kalra, Biodegradable polymers for the environment, Science 297 (2002) 803–807, http://dx.doi.org/10.1126/science.297.5582.803.

[11] S. Walker, J. Rueben, T.V. Volkenburg, S. Hemleben, C. Grimm, J. Simonsen, Y. Mengüç, Using an environmentally benign and degradable elastomer in soft robotics, Int. J. Intell. Robot. Appl. 1 (2017) 124–142, http://dx.doi.org/10.1007/s41315-017-0016-8.

[12] J. Muller, C. González-Martínez, A. Chiralt, Combination of poly(lactic) acid and starch for biodegradable food packaging, Materials 10 (2017) 952, http://dx.doi.org/10.3390/ma10080952.

[13] Science to enable sustainable plastics, 2020, Royal Society of Chemistry, https://www.rsc.org/new-perspectives/sustainability/progressive-plastics/. (Accessed 18 June 2020).

[14] F. Gallo, C. Fossi, R. Weber, D. Santillo, J. Sousa, I. Ingram, A. Nadal, D. Romano, Marine litter plastics and microplastics and their toxic chemicals components: the need for urgent preventive measures, Environ. Sci. Eur. 30 (2018) 13, http://dx.doi.org/10.1186/s12302-018-0139-z.

[15] A.-C. Albertsson, M. Hakkarainen, Designed to degrade, Science 358 (2017) 872–873, http://dx.doi.org/10.1126/science.aap8115.

[16] A. Barański, D. Dutka, R. Dziembaj, A. Konieczna-Molenda, J.M. Łagan, Effect of relative humidity on the degradation rate of cellulose, Methodol. Stud. Restaurator. 25 (2004) http://dx.doi.org/10.1515/REST.2004.68.

[17] T.P. Haider, C. Völker, J. Kramm, K. Landfester, F.R. Wurm, Plastics of the future? The impact of biodegradable polymers on the environment and on society, Angew. Chem. Int. Ed. 58 (2019) 50–62, http://dx.doi.org/10.1002/anie.201805766.

[18] A. Göpferich, Polymer bulk erosion, Macromolecules 30 (1997) 2598–2604, http://dx.doi.org/10.1021/ma961627y.

[19] F. von Burkersroda, L. Schedl, A. Göpferich, Why degradable polymers undergo surface erosion or bulk erosion, Biomaterials 23 (2002) 4221–4231, http://dx.doi.org/10.1016/S0142-9612(02)00170-9.

[20] N. Murthy, S. Wilson, J.C. Sy, Biodegradation of polymers, in: Polym. Sci. Compr. Ref., Elsevier, 2012, pp. 547–560, http://dx.doi.org/10.1016/B978-0-444-53349-4.00240-5.

[21] A. Gijpferich, Mechanisms of polymer degradation and erosion, 17, 1996, p. 12.

[22] E. Orowan, The fatigue of glass under stress, Nature 154 (1944) 341–343.

[23] S.M. Wiederhorn, Moisture assisted crack growth in ceramics, Int. J. Fract. Mech. 4 (1968) http://dx.doi.org/10.1007/BF00188945.

[24] Stress Corrosion Cracking of Aluminum Alloys, SpringerLink, 2020, https://link.springer.com/article/10.1007/BF02672284. (Accessed 18 June 2020).

[25] K. Sieradzki, R.C. Newman, Brittle behavior of ductile metals during stress-corrosion cracking, Philos. Mag. A. 51 (1985) 95–132, http://dx.doi.org/10.1080/01418618508245272.

[26] M. Braden, A.N. Gent, The attack of ozone on stretched rubber vulcanizates. I. The rate of cut growth, J. Appl. Polym. Sci. 3 (1960) 90–99, http://dx.doi.org/10.1002/app.1960.070030713.

[27] X. Yang, J. Yang, L. Chen, Z. Suo, Hydrolytic crack in a rubbery network, Extreme Mech. Lett. 31 (2019) 100531, http://dx.doi.org/10.1016/j.eml.2019.100531.

[28] S.R. Dupont, F. Novoa, E. Voroshazi, R.H. Dauskardt, Decohesion kinetics of PEDOT:PSS conducting polymer films, Adv. Funct. Mater. 24 (2014) 1325–1332, http://dx.doi.org/10.1002/adfm.201302174.

[29] Y. Wang, G.A. Ameer, B.J. Sheppard, R. Langer, A tough biodegradable elastomer, Nat. Biotechnol. 20 (2002) 602–606, http://dx.doi.org/10.1038/nbt0602-602.

[30] M.J. Kim, M.Y. Hwang, J. Kim, D.J. Chung, Biodegradable and elastomeric poly(glycerol sebacate) as a coating material for nitinol bare stent, BioMed Res. Int. 2014 (2014) 1–7, http://dx.doi.org/10.1155/2014/956952.

[31] Q. Chen, S. Liang, G.A. Thouas, Synthesis and characterisation of poly(glycerol sebacate)-co-lactic acid as surgical sealants, Soft Matter. 7 (2011) 6484–6492, http://dx.doi.org/10.1039/C1SM05350G.

[32] X. Li, A.T.-L. Hong, N. Naskar, H.-J. Chung, Criteria for quick and consistent synthesis of poly(glycerol sebacate) for tailored mechanical properties, Biomacromolecules 16 (2015) 1525–1533, http://dx.doi.org/10.1021/acs.biomac.5b00018.

[33] R.S. Rivlin, A.G. Thomas, Rupture of rubber. I., Rupture of rubber. i characteristic energy for tearing, J. Polym. Sci. 10 (1953) 291–318, http://dx.doi.org/10.1002/pol.1953.120100303.

[34] Z. Wang, C. Xiang, X. Yao, P. Le Floch, J. Mendez, Z. Suo, Stretchable materials of high toughness and low hysteresis, Proc. Natl. Acad. Sci. 116 (2019) 5967–5972, http://dx.doi.org/10.1073/pnas.1821420116.

[35] G.J. Lake, Fatigue and fracture of elastomers, Rubber Chem. Technol. 68 (1995) 435–460, http://dx.doi.org/10.5254/1.3538750.

[36] C. Chen, Z. Wang, Z. Suo, Flaw sensitivity of highly stretchable materials, Extreme Mech. Lett. 10 (2017) 50–57, http://dx.doi.org/10.1016/j.eml.2016.10.002.

[37] G.J. Van Amerongen, The permeability of different rubbers to gases and its relation to diffusivity and solubility, J. Appl. Phys. 17 (1946) 972–985, http://dx.doi.org/10.1063/1.1707667.

[38] Y. Ding, Q. Xiao, R.H. Dauskardt, Molecular design of confined organic network hybrids with controlled deformation rate sensitivity and moisture resistance, Acta Mater. 142 (2018) 162–171, http://dx.doi.org/10.1016/j.actamat.2017.09.060.